

## THE REDSHIFT OF A LENSING GALAXY IN PMN J0134–0931

PATRICK B. HALL,<sup>1,2</sup> GORDON T. RICHARDS,<sup>3</sup> DONALD G. YORK,<sup>4,5</sup> CHARLES R. KEETON,<sup>4</sup> DAVID V. BOWEN,<sup>1</sup> DONALD P. SCHNEIDER,<sup>3</sup> DAVID J. SCHLEGEL,<sup>1</sup> J. BRINKMANN<sup>6</sup>

## ABSTRACT

The Sloan Digital Sky Survey (SDSS) automatically targeted as a quasar candidate the recently discovered, gravitationally lensed, extremely reddened  $z = 2.2$  quasar PMN J0134–0931. The SDSS spectrum exhibits Ca II absorption at  $z = 0.76451$ , which we identify as the redshift of a lensing galaxy. *Hubble Space Telescope* imaging shows that components CDE of the system are significantly redder than components A or B and detects faint galaxy emission between D and A+B. The redshift of the dust responsible for the reddening remains unconstrained with current data. However, we outline a model wherein lensing and differential reddening by a  $z = 0.76451$  galaxy pair can entirely explain this system.

*Subject headings:* gravitational lensing — dust, extinction — quasars: individual (PMN J0134–0931)

## 1. INTRODUCTION

The Sloan Digital Sky Survey<sup>7</sup> (SDSS; York et al. 2000) is using a drift-scanning imaging camera (Gunn et al. 1998) to image  $10^4 \text{ deg}^2$  of sky on the SDSS *ugriz* AB magnitude system (Fukugita et al. 1996; Hogg et al. 2001; Smith et al. 2002). Two multi-fiber, double spectrographs on a dedicated 2.5m telescope are used to obtain spectra for  $\sim 10^6$  galaxies to  $r = 17.8$  and  $\sim 10^5$  quasars to  $i = 19.1$  ( $i = 20.2$  for  $z > 3$  candidates). As discussed in Richards et al. (2002), quasar candidates are targeted for spectroscopy because they are outliers from the stellar locus or because they are unresolved objects with radio emission detected by the FIRST survey (Becker, White, & Helfand 1995). Due to these inclusive criteria and its area and depth, the SDSS is effective at finding quasars with unusual properties and colors (Hall et al. 2002).

Quasars heavily reddened by dust form one population of quasars with ‘unusual’ colors, at least for optically selected, magnitude limited samples. Recently, Gregg et al. (2002), hereafter G02, reported on two heavily reddened quasars from a survey of FIRST radio sources with red counterparts in the Two-Micron All-Sky Survey (Skrutskie et al. 1997). One of these — PMN J0134–0931 — is gravitationally lensed, as discovered independently by G02 and Winn et al. (2002), hereafter W02.

W02 identify six radio components of J0134-0931, five of which have the same spectral slope (not measurable for the faintest component, F), and two of which (C and E) have lower surface brightnesses than the others. W02 present two lens models. In one, J0134-0931 is a six-image lens, with C and E differentially broadened by interstellar scattering (Jones et al. 1996). This model requires more than one lensing galaxy and even then might not reproduce the image configuration. In the second, despite the similar spectral slopes of all the radio components, C and

E are a foreground object or objects while A+B and D+F are the double images of a core+jet source. This model requires almost perfect source-lens alignment to match the flux ratios. However, components A, B and D+F (the D+F separation is only  $0''.05$ ) have near-IR (NIR) counterparts with very different flux ratios than in the radio. More data are clearly needed for a viable lens model.

J0134-0931 was independently targeted as a quasar candidate in the SDSS. Here we investigate this system further using SDSS and *Hubble Space Telescope* (*HST*) data.

## 2. SDSS DATA ON PMN J0134–0931

J0134-0931 was bright enough in the SDSS for consideration as a high-redshift quasar candidate (Table 1). It qualifies as such a candidate because it has  $g^* - r^* = 2.26$ , redder than the  $g^* - r^* > 2.1$  threshold used as part of the  $z \geq 3.6$  quasar candidate selection (Richards et al. 2002).

The SDSS obtained spectra of J0134-0931 on UT Aug. 26 and Sep. 26, 2001, for a total exposure of 125.1 minutes. The inverse-variance-weighted average spectrum, smoothed by a seven pixel boxcar, is shown in Figure 1. Broad Mg II emission from the quasar is seen, along with weak C III] and C IV. The  $\lambda \lesssim 3900 \text{ \AA}$  rise is spurious: it is within the range of observed sky fiber residuals, and photometry shows this object is much fainter in  $u$  ( $< 3900 \text{ \AA}$ ) than in  $g$  ( $3900\text{--}5400 \text{ \AA}$ ). Cross-correlation with the SDSS composite quasar of Vanden Berk et al. (2001) yields a redshift  $z = 2.225 \pm 0.006$ , which is  $840 \text{ km s}^{-1}$  higher than G02’s  $z = 2.216$  based on the optical/NIR spectrum.

Also present in the SDSS spectrum are two absorption lines near  $7000 \text{ \AA}$ . Both lines are detected in each of the two SDSS spectra, and can in fact be seen in Figure 3 of G02. The wavelengths match those of Ca II H&K at  $z = 0.76451 \pm 0.00016$  and do not match intervening Fe II or Mg II. The absorption is resolved, with intrinsic  $\sigma_v = 220 \pm 40 \text{ km s}^{-1}$ , and the EW ratio  $0.55 \pm 0.16$  is con-

<sup>1</sup> Princeton University Observatory, Princeton, NJ 08544-1001

<sup>2</sup> Departamento de Astronomía y Astrofísica, Facultad de Física, Pontificia Universidad Católica de Chile, Casilla 306, Santiago 22, Chile

<sup>3</sup> Department of Astronomy and Astrophysics, The Pennsylvania State University, University Park, PA 16802

<sup>4</sup> Department of Astronomy and Astrophysics, The University of Chicago, 5640 S. Ellis Ave., Chicago, IL 60637

<sup>5</sup> Enrico Fermi Institute, The University of Chicago, 5640 S. Ellis Ave., Chicago, IL 60637

<sup>6</sup> Apache Point Observatory, P.O. Box 59, Sunspot, NM 88349-0059

<sup>7</sup> The SDSS Web site is <http://www.sdss.org/>.

sistent with predominantly unsaturated absorption (EW ratio 0.5).<sup>8</sup> The absorption is very strong, with rest-frame  $EW_{\text{CaII,K}} = 5.3 \pm 0.5 \text{ \AA}$ , vs. typical  $EW < 1 \text{ \AA}$  seen in the Galaxy and extragalactic Mg II absorption systems (§ IV of Briggs et al. 1985). The only objects with similar values are the lens B 0218+357 (Browne et al. 1993) and the ultra-luminous IR galaxies of Rupke, Veilleux, & Sanders (2002).

The smoothed, coadded spectrum shows *apparent* absorption and emission, respectively, near the expected positions of Mg II and [O II] at  $z = 0.7645$ . However, inspection of both unsmoothed spectra shows that neither feature was obviously present on both spectra, and that other apparent narrow emission and absorption features (e.g., at 8300–8900 Å) are sky line subtraction residuals or lie near sky lines, where the noise is higher. Thus we do not believe there is any significant, narrow absorption or emission in the SDSS spectrum, except for Ca II.

### 3. HST DATA ON PMN J0134–0931

*HST* WFPC2 images of J0134-0931 in *F814W* and *F555W* were retrieved from MAST.<sup>9</sup> In each filter, two undithered 21.7 minute exposures were coadded with iterative cosmic ray rejection. Only components ABD are clearly detected in *F814W* (Figure 2, center panel), and only A and B in *F555W* (not shown). Components CE are not present at the flux ratios relative to A and B seen in the NIR or radio, and component D is also unexpectedly faint. Using IRAF QPHOT and  $0''.092$  (2 pixel) radius apertures, we measure A:B:D flux ratios accurate to  $\sim 5\%$  of 0.93:1:<0.025 in  $V_{555W}$  and 1.45:1:0.044 in  $I_{814W}$ , vs. 1.11:1:0.28 in  $K'$  and 4.05:1:0.76 at 3.6 cm (see G02).

To determine how much of the low-surface-brightness emission around J0134-0931 is due to the point-spread functions (PSFs) of A+B, we used two unsaturated stars on the planetary camera. Each star was rescaled to the same flux as component A, B or D in a  $0''.092$  radius. These three scaled images were then shifted by integer pixels to the positions of the corresponding components and coadded. The averaged PSF image of the two stars is shown in the left panel of Figure 2, and the PSF-subtracted image of J0134-0931 in the right panel. The circles show areas with significant PSF subtraction residuals. We see possible emission at the position of component E, and a definite excess of low-surface-brightness emission between components D and A+B. Accurately determining the centroid and morphology of the extended emission will require a subpixel shift analysis of the *HST* images, since our PSF subtraction residuals prevent detection of emission within  $\lesssim 0''.25$  of A+B. (Note that G02 did find possible emission midway between components A and D in their deconvolved  $K'$  image.) The total extended flux we can detect is  $\sim 4.1\%$  of the  $0''.092$  radius  $I_{814W}$  flux of component B.

### 4. WHERE IS THE DUST?

We estimate the redshift and amount of dust reddening in J0134-0931 by reddening a composite quasar constructed from the SDSS Early Data Release quasar cata-

log (Schneider et al. 2002), following Vanden Berk et al. (2001). We minimized the  $\chi^2$  between the reddened composite and the unsmoothed SDSS spectrum of J0134-0931 (after correcting the latter for Galactic extinction using IRAF DEREDDEN), accounting for both the observed errors on the fluxes in each pixel and the rms variation of the composite quasar at the corresponding rest-frame wavelength. We considered only the SMC reddening curve (Pei 1992), since G02 found that it was the only empirical curve which could reasonably match the spectrum of J0134-0931.

If the dust is at the quasar redshift, we find  $E(B-V) = 0.670 \pm 0.015$ , with  $\chi^2_\nu = 1.073$ . With  $R_V = 2.93$  (Pei 1992), this corresponds to  $A_V = 1.96 \pm 0.05$ , in good agreement with G02 ( $A_V = 2.1$ ). If the dust is at  $z = 0.7645$ , we find  $E(B-V) = 1.315 \pm 0.025$  with  $\chi^2_\nu = 1.041$ . This corresponds to  $A_V = 3.85 \pm 0.08$ , lower than the  $A_V = 4.5$  found by G02 when they assumed  $z_{\text{lens}} = 0.5$ .

Both fits have  $\chi^2_\nu \simeq 1$ , but the goodness of fit parameter (Press et al. 1992) shows that dust at  $z = 0.7645$  is formally a better fit. We synthesized *ugrizBVRIJHK<sub>s</sub>* photometry of the best-fit reddened composite quasars to see if the fits to the optical spectrum matched the NIR photometry. Figure 3 shows that they do not, and that dust at  $z=0.7645$  gives a worse fit. For SMC reddening, J0134-0931 is as bright in  $J$  as expected from its optical colors, but not as red in  $J-K<sub>s</sub>$ . Variability between the NIR and optical imaging epochs cannot explain this, as quasars are bluer when they are brighter (Trèvese & Vagnetti 2002).

### 5. A PLAUSIBLE MODEL FOR PMN J0134–0931

The SDSS has detected extremely strong Ca II absorption at  $z = 0.76451 \pm 0.00016$  in the spectrum of the reddened, gravitationally lensed  $z = 2.225$  quasar PMN J0134–0931. We identify this as absorption from a gas-rich lensing galaxy. Current data do not allow us to discriminate between dust reddening at the source or in the lens. However, *HST* imaging shows that component D is  $\simeq 2^m.3$  redder in  $I_{814W} - K'$  than the already heavily reddened components A and B which dominate the flux in the SDSS spectrum. Spectroscopy of component D alone is lacking, but the radio data of W02 are strong evidence that at least A, B and D are images of a single quasar. If so, differential reddening in an intervening galaxy seems the most plausible explanation for the colors of components D and B (and probably C and E). *HST* has also detected faint emission between A+B and D. If the  $z=0.7645$  galaxy differentially reddens component D, such  $I_{814W}$ -band emission, redward of the redshifted 4000 Å break, is expected.

Note that the strong Ca II absorption indicates a high column density of gas at  $z = 0.7645$ , but not necessarily of dust, because Ca II is easily depleted (Robertson et al. 1988). Thus, differential reddening at  $z = 0.7645$  is not *required*, though it is of course possible for physically unrelated dust reddening and Ca II absorption to occur along the same sightlines at  $z = 0.7645$ . The maximum Ca II absorption depth of  $\sim 75\%$  of the continuum indicates that largely unsaturated absorption is present in both A and B,

<sup>8</sup> All uncertainties calculated from resampling a two-gaussian fit to the data, constrained to one FWHM and the Ca II wavelength ratio, with IRAF NGAUSSFITS. The Image Reduction and Analysis Facility is distributed by NOAO, operated by AURA, Inc., under contract to the NSF.

<sup>9</sup> G.O. #9133, P.I. Falco. MAST is the Multimission Archive at STScI, which is operated by AURA, Inc., under NASA contract NAS5-26555.

<sup>10</sup> Both A and B being images of the quasar argues against W02's model wherein they are images of a core and jet, as the optical source would have to be larger than the core+jet. This model would be ruled out if detailed analysis of the *HST* data showed no optical arc from A to B.

since they contribute to the optical light in a ratio  $\sim 3:2$ .<sup>10</sup>

One simple hypothesis is that J0134-0931 is lensed by two galaxies (see below), at least one at  $z = 0.7645$ , wherein differential scatter broadening produces the larger radio sizes of C and E while differential extinction makes components BCDE much redder than A. (Dust at the source may still play a role, but cannot produce significant differential reddening between components.) Differential reddening is seen in two-thirds of lenses (Falco et al. 1999), and was suggested by G02 as a possible explanation for the red  $J - K'$  of component D compared to A or B. Note that the dust column densities in front of CDE must be large enough to produce  $\Delta E(B - V) \gtrsim 0.27$  for  $z_{dust} < 2.225$  ( $\Delta E(B - V) \gtrsim 0.56$  at  $z = 0.7645$ ), which occurs in only  $\sim 10\%$  of lens sightlines (Falco et al. 1999).

Even though we and G02 have shown that SMC, LMC or MW reddening is a poor fit to the photometry of J0134-0931, given the diversity of astrophysical extinction curves (Savage & Mathis 1979), in principle simple differential extinction at  $z = 0.7645$  — with an extinction curve steeper than the SMC's at  $\lambda \lesssim 5000 \text{ \AA}$  — could still explain the relative fluxes of all components except for A. The A:B ratio is 4:1 in the radio and 1.1:1 at  $K'$ . Explaining this difference via microlensing amplification of the radio but not the optical source in A can be ruled out by the lack of variability in the total radio flux over almost 20 yr (Figure 2 of W02). If this difference was due to differential extinction with the same extinction curve as the other components, the observed optical A:B ratio would be  $\ll 1$ , which is not the case. One possible explanation for A is a range of reddenings across its sightline through an intervening galaxy. If 75% of A's flux was reddened as much as component D, that reddened flux would dominate at  $K'$  while the less reddened 25% would dominate at shorter wavelengths. Such reddening gradients are seen in some quasars (Hall et al. 2002, § 5.3), but the  $\lesssim 0.1$  pc size scale over which this reddening gradient must occur is much smaller than the minimum cloud diameter of  $\sim 3$  pc inferred by Frye, Welch, & Broadhurst (1997) for the lens in PKS 1830–211.

To explain the image configuration in the differential reddening model, we suggest that D+F is a *single* image, showing the true source morphology of a core and weak jet. and that the jet images corresponding to the core images A and B are missing because the source plane positions of the core and jet yield different numbers of multiple images. A two-deflector version of the five-deflector system in Figure 2 of Keeton (2002) can produce five bright images in roughly the J0134-0931 configuration, but only two images of a nearby jet (for certain position angles). This model is quite testable: it requires a faint component G near C which is a parity-reversed image of F; E and C+G to be broadened by interstellar scattering (and to a lesser extent

A, since its radio surface brightness is lower than B); and two lens galaxies, one near E and one between A and D, both locations at which G02 saw possible  $K'$  emission.

As for other tests, high spatial resolution NIR images and spectra could yield colors and positions for all deflectors and components, determine which are images of the quasar (via  $H\alpha$ ), and measure extinction curves (Falco et al. 1999). Absolute and differential reddenings at  $z = 0.7645$  can be constrained by looking for molecular absorption in the radio components (Frye et al. 1997). A high signal-to-noise ratio spectrum could constrain the dust location via K I,  $C_2$ , Li I or CN absorption directly from dusty gas.

This work shows that the SDSS can contribute to the study of reddened quasars. G02 state that 'such objects will be entirely missed by standard ... optical quasar surveys', yet the SDSS selected J0134-0931, by its color, as a quasar candidate. Such reddened, low- $z$  quasars have colors similar to normal high- $z$  quasars (Richards et al. 2001), and thus SDSS selects them a magnitude deeper than unreddened low- $z$  quasars. Also, J0134-0931 would have been selected as a low- $z$  quasar candidate via both its colors and FIRST, had it been only  $0^m523$  brighter in  $i^*$ . However, unlensed objects as red as J0134-0931 will be rare at the magnitude limits of the SDSS, which probes only the top of the luminosity function for the reddest objects. Thus, since AGN with reddenings larger than that of J0134-0931 exist, a full understanding of the prevalence and properties of reddened quasars will require multiwavelength observations. Nonetheless, the large area of the SDSS will enable study of the reddening distribution to at least  $E(B - V) \simeq 0.65$ . In G02's terminology, the SDSS is not a 'standard' optical quasar survey, and is quite sensitive to reddened quasars (Richards et al. 2002, in prep.).

We thank the anonymous referee for useful comments. The SDSS is a joint project of the University of Chicago, Fermilab, the Institute for Advanced Study, the Japan Participation Group, The Johns Hopkins University, Los Alamos National Laboratory, the Max-Planck-Institute for Astronomy, the Max-Planck-Institute for Astrophysics, New Mexico State University, Princeton University, the United States Naval Observatory, and the University of Washington. Apache Point Observatory, site of the SDSS telescopes, is operated by the Astrophysical Research Consortium. Funding for the SDSS has been provided by the Alfred P. Sloan Foundation, SDSS member institutions, the National Aeronautics and Space Administration, the National Science Foundation, the U.S. Department of Energy, the Japanese Monbukagakusho, and the Max Planck Society. P. B. H. is supported by FONDECYT grant 1010981, and D. P. S. & G. T. R. by NSF grant 99-00703.

## REFERENCES

- Becker, R., White, R., & Helfand, D. 1995, ApJ, 450, 559  
 Briggs, F., Wolfe, A., Turnshek, D., & Schaeffer, J. 1985, ApJ, 293, 387  
 Browne, I., Patnaik, A., Walsh, D., & Wilkinson, P. 1993, MNRAS, 263, L32  
 Falco, E., Impey, C., Kochanek, C., Lehár, J., McLeod, B., Rix, H.-W., Keeton, C., Muñoz, J., et al., 1999, ApJ, 523, 617  
 Frye, B., Welch, W., & Broadhurst, T. 1997, ApJ, 478, L25  
 Fukugita, M., Ichikawa, T., Gunn, J., Doi, M., Shimasaku, K., & Schneider, D. 1996, AJ, 111, 1748  
 Gregg, M., Lacy, M., White, R., Gilkman, E., Helfand, D., Becker, R., & Brotherton, M. 2002, ApJ, 564, 133  
 Gunn, J., Carr, M., Rockosi, C., Sekiguchi, M., Berry, K., Elms, B., de Haas, E., Ivezić, Ž., et al., 1998, AJ, 116, 3040  
 Hall, P., Anderson, S., Strauss, M., York, D., Richards, G., Fan, X., Knapp, G., Schneider, D., et al., 2002, ApJS, in press  
 Hogg, D., Finkbeiner, D., Schlegel, D., & Gunn, J. 2001, AJ, 122, 2129  
 Jones, D., Preston, R., Murphy, D., Jauncey, D., Reynolds, J., Tzioumis, A., King, E., McCulloch, P., et al., 1996, ApJ, 470, L23

- Keeton, C. 2002, ApJ, submitted (astro-ph/0102340)  
 Lupton, R., Gunn, J., & Szalay, A. 1999, AJ, 118, 1406  
 Pei, Y. 1992, ApJ, 395, 130  
 Pier, J., Munn, J., Hindsley, R., Hennessy, G., Kent, S., Lupton, R., & Ivezić, Z. 2002, AJ, submitted  
 Press, W., Teukolsky, S., Vetterling, W., & Flannery, B. 1992, Numerical recipes in FORTRAN: The art of scientific computing (Cambridge: University Press, 2nd ed.), 657  
 Richards, G., Fan, X., Newberg, H., Strauss, M., Vanden Berk, D., Schneider, D., Yanny, B., Boucher, A., et al., 2002, AJ, 123, 2945  
 Richards, G., Weinstein, M., Schneider, D., Fan, X., Strauss, M., Vanden Berk, D., Annis, J., Burles, S., et al., 2001, AJ, 122, 1151  
 Robertson, J., Morton, D., Blades, J., York, D., & Meyer, D. 1988, ApJ, 325, 635  
 Rupke, D., Veilleux, S., & Sanders, D. 2002, ApJ, 570, 588  
 Savage, B. & Mathis, J. 1979, ARA&A, 17, 73  
 Schneider, D., Richards, G., Fan, X., Hall, P., Strauss, M., Vanden Berk, D., Gunn, J., Newberg, H., et al., 2002, AJ, 123, 567  
 Skrutskie, M., Schneider, S., Stiening, R., Strom, S., Weinberg, M., Beichman, C., Chester, T., Cutri, R., et al., 1997, in The Impact of Large Scale Near-IR Sky Surveys, eds. F. Garzon et al., (Dordrecht: Kluwer), 25  
 Smith, J., Tucker, D., Kent, S., Richmond, M., Fukugita, M., Ichikawa, T., Ichikawa, S., Jorgensen, A., et al., 2002, AJ, 123, 2121  
 Stoughton, C., Lupton, R., Bernardi, M., Blanton, M., Burles, S., Castander, F., Connolly, A., Eisenstein, D., et al., 2002, AJ, 123, 485  
 Trèvese, D. & Vagnetti, F. 2002, ApJ, 564, 624  
 Vanden Berk, D., Richards, G., Bauer, A., Strauss, M., Schneider, D., Heckman, T., York, D., Hall, P., et al., 2001, AJ, 122, 549  
 Winn, J., Lovell, J., Chen, H., Fletcher, A. Hewitt, J., Patnaik, A., & Schechter, P. 2002, ApJ, 564, 143  
 York, D., Adelman, J., Anderson, J., Anderson, S., Annis, J., Bahcall, N., Bakken, J., Barkhouser, R., et al., 2000, AJ, 120, 1579

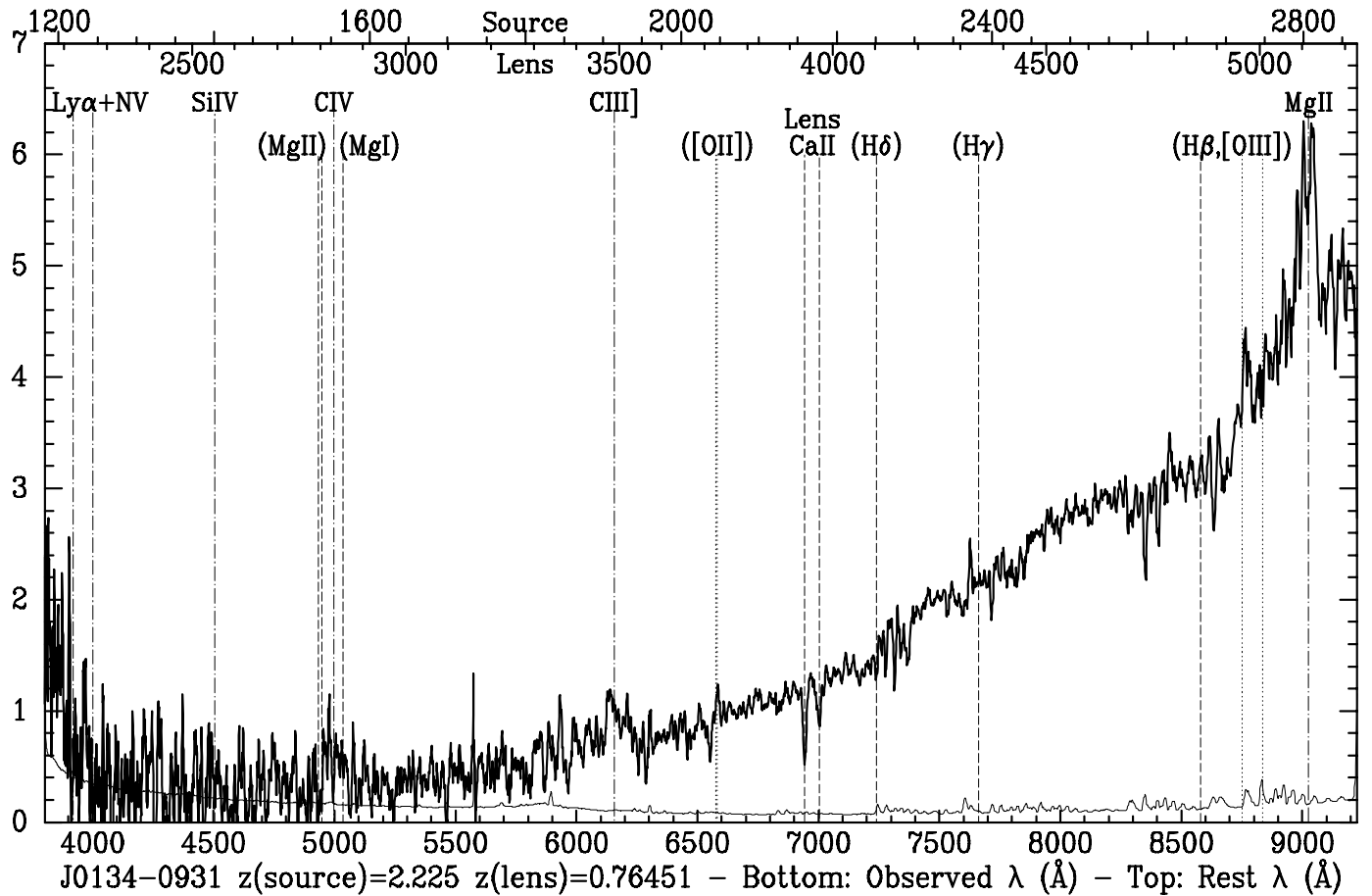


FIG. 1.— The coadded SDSS spectrum ( $\lambda/\delta\lambda \approx 1800$ ) of J0134-0931, smoothed by a seven pixel boxcar. The noise level is shown by the thin line across the bottom of the Figure. The abscissa is  $F_\lambda$  in units of  $10^{-17}$  ergs  $\text{cm}^{-2}$   $\text{s}^{-1}$   $\text{\AA}^{-1}$ . Observed wavelengths (in  $\text{\AA}$ ) are shown below the bottom axis, and wavelengths in the rest frame of the source (lens) above (below) the top axis. Dash-dot lines show the expected wavelengths of broad emission lines at  $z = 2.225$ . Dashed lines show CaII absorption at  $z = 0.7645$  as well as the expected wavelengths of strong lines from H and Mg at  $z = 0.76451$ . Dotted lines show the expected wavelengths of narrow [OII] and [OIII] emission at  $z = 0.76451$ .

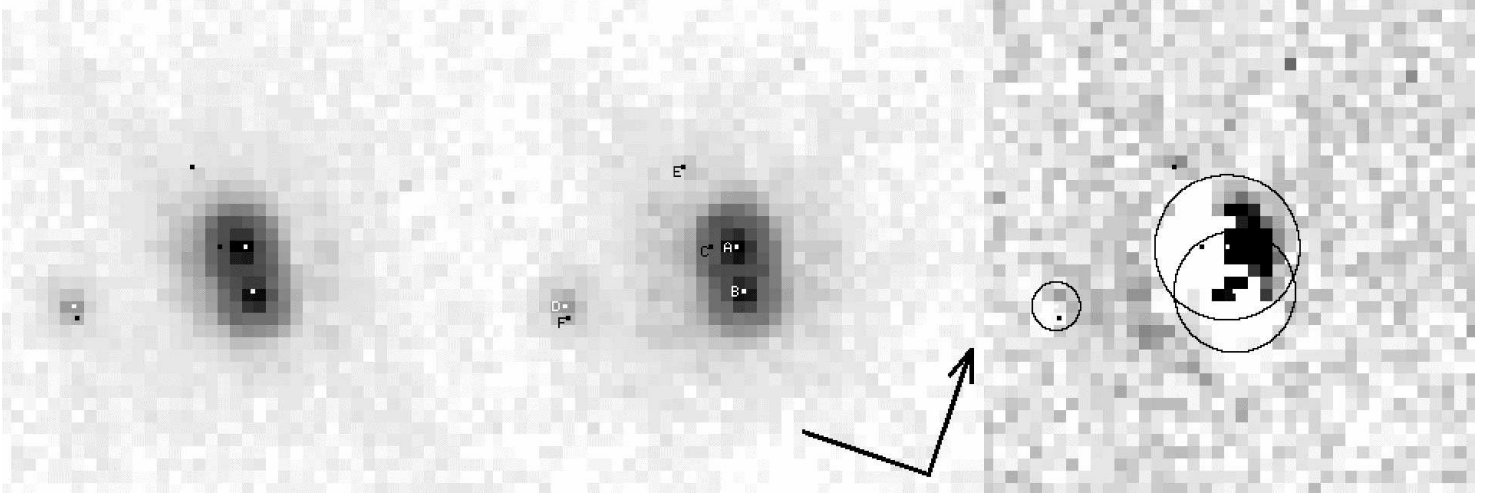


FIG. 2.— The center panel shows the *HST F814W* planetary camera image of J0134-0931 ( $0''.046/\text{pixel}$ ). North (with arrow) and East are shown with bars  $0''.50$  long. The six radio components are labelled: components whose positions were measured in the *HST* image are white, and those whose positions were inferred from radio data are black. The left panel shows a PSF image containing only the emission expected from point sources at A, B and D, displayed on the same  $\log(\text{square root})$  intensity scale as the raw image. All panels are reverse contrast (dark areas are emission). The right panel shows the residuals after subtraction of the PSF image, displayed on a linear intensity scale. The circles outline regions dominated by PSF subtraction residuals. The integer pixel shifts used to make the PSF image inadequately account for the subpixel centroids of A, B and D. Nonetheless, beyond the extent of these residuals, there is faint but real emission between D and A+B.

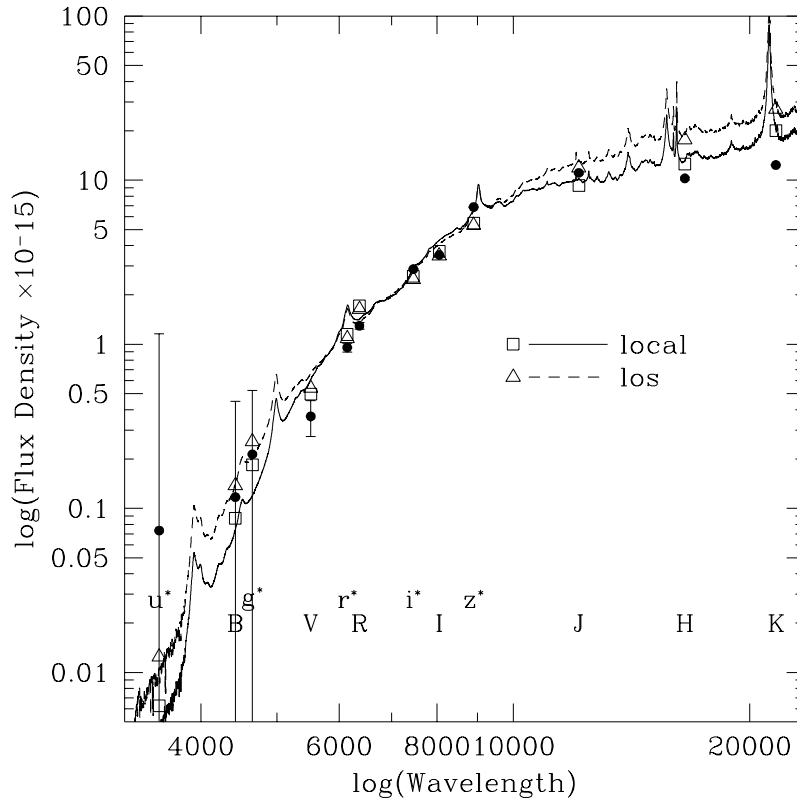


FIG. 3.— ‘Best’ fits of the SDSS EDR composite quasar reddened by  $E(B - V) = 0.67$  of dust at the quasar redshift (‘local’) and by line-of-sight  $E(B - V) = 1.3$  at the lens redshift (‘los’) to all published photometry of J0134-0931 (filled points with error bars). (Since components A and B contribute essentially all the optical light but only  $\sim 84.5\%$  and  $\sim 81.5\%$  of the  $J$  and  $K'$  emission (G02), and by interpolation 83% in  $H$ , we reduced the 2MASS magnitudes accordingly for a consistent comparison.) The normalizations have been adjusted to minimize the  $\chi^2$  compared to the optical/NIR photometry. Neither fit is statistically acceptable, but dust at the lens redshift (which best fits the optical spectrum) is a considerably worse fit to the NIR photometry than dust at the quasar redshift.

TABLE 1  
SDSS DATA ON PMN J0134–0931

J2000 Coordinates	Source Redshift	Lens Redshift	SDSS Photometry on UT Sep. 27, 2000					Galactic $E(B-V)$
			$u^* \pm \sigma_{u^*}$	$g^* \pm \sigma_{g^*}$	$r^* \pm \sigma_{r^*}$	$i^* \pm \sigma_{i^*}$	$z^* \pm \sigma_{z^*}$	
013435.66–093102.9	2.225±0.006	0.76451±0.00016	25.34±1.08	23.54±0.31	21.28±0.06	19.65±0.03	18.30±0.03	0.0305

Note. — The SDSS coordinates should be good to  $\sim 0''.060$  rms each for an object of this  $i$  magnitude (Pier et al. 2002). Pending the final definition of the SDSS photometric system, the magnitudes are preliminary and are denoted by  $u^* g^* r^* i^* z^*$  (see §4.5 of Stoughton et al. 2002). All SDSS magnitudes are asinh magnitudes (Lupton, Gunn, & Szalay 1999), with zero-flux magnitudes 24.63, 25.11, 24.80, 24.36 and 22.83 respectively.